 CMES, vol.63, no.2, pp.101-115, 2010

An Analysis of the Transient Heat Conduction for Plates with the Functionally Graded Material Using the Hybrid Numerical Method

J.H. Tian[1,2], X. Han[2], S.Y. Long[2], G.Y. Sun[2], Y. Cao[1] and G.Q. Xie[3]

Abstract: A transient heat conduction analysis of the functionally graded material (FGM) plates has been investigated based on the hybrid numerical method (HNM). HNM combines the layer element method with the method of Fourier transforms and proves to be efficient and reliable. The FGM plates are infinite large and the material properties vary continuously through thickness. The transient heat source acted on the FGM plates. The temperature distribution of the FGM plates is obtained in different time and different position. Some useful results for transient heat conduction are shown in figures. Applications of HNM to transient heat conduction are firstly presented a new way for studying the transient heat conduction problems.

Keywords: Functionally graded material; transient heat conduction; hybrid numerical method

1 Introduction

Functionally graded material (FGM) has been developed as a new material that is adaptable for a super-high-temperature environment. Temperature change often represents a significant factor, and often induces the failure of FGM. So investigating the heat problems of the FGM plates is very necessary.

Researchers have presented many methods to investigate heat problems of FGM. Ootao and Tanigawa (2002) were concerned with the theoretical treatment of transient thermal stress problem involving an angle-ply laminated cylindrical panel

[1] School of Mechatronic Engineering, Xi'an Technological University, Xi'an,710032,China, Email: carl8@163.com

[2] State Key Laboratory of Advanced Design and Manufacturing for Vehicle Body, Hunan University, Changsha, 410082, China

[3] Civil Engineering College of Hunan University of Science and technology, Xiangtan ,411201,China

consisting of an oblique pile of layers having orthotropic material properties due to nonuniform heat supply in the circumferential direction. Savoia and Reddy (1995) presented results of the stress analysis of multilayered plates subject to thermal and mechanical loads in the context of the three-dimensional quassi-static theory of thermoelasticity. Cheng and Batra (2000), Reddy and Cheng (2001) used the asymptotic expansion method to study the three-dimensional thermoelastic deformations of functionally graded elliptic and rectangular plates, respectively. Vel and Batra (2002,2003) presented exact three-dimensional solutions for the steady-state and quasi-static transient thermoelastic response of functionally graded thick plates with an arbitrary variation of material properties in the thickness direction. Qian et al. (2004), Qian and Batra (2004) obtained results for the steady-state and transient thermoelastic response of functionally graded plates using the meshless local Petrov–Galerkin method that agrees with the exact solution of Vel and Batra (2002,2003). Sladek et al. (2008a, 2008b) applied a meshless local Petrov-Galerkin (MLPG) method into solving problems of Reissner-Mindlin shells under thermal loading and also proposed a meshless method based on the local Petrov-Galerkin approach to obtain the solution of steady-state and transient heat conduction problems in a continuously nonhomogeneous anisotropic medium. Chein-Shan Liu (2008) treated inverse thermal stress problems using the Lie-group shooting method through an internal temperature measurement. Lutz and Zimmerman presented the exact solutions for one-dimensional thermal stresses of functionally graded cylinder (1996) and sphere (1999) whose elastic moduli and thermal expansion coefficients vary linearly along radius.

Recently, Liu (2002) proposed an efficient and reliable method called HNM. This method combined efficiency of the finite element method and accuracy of the analytical method. It had been applied to solve displacement response problems and proved to be validity. Tian et al.(2009) expanded HNM to investigate the heat conduction problem of FGM plates and obtained useful results. In this paper, the analysis of the transient heat conduction for plates with the functionally graded material is presented using HNM.

2 Heat conduction formulation based on HNM

Consider a plate with the functionally graded material that has nonhomogeneous thermal and mechanical properties along the thickness direction as shown in Fig.1. Its thickness is represented by H. Here, assume that the plate is initially at zero temperature and is suddenly heated from the middle line y axis of the upper surface by the surrounding medium with relative heat transfer coefficient α, and assume that the heat source is throughout the y-direction. Then this problem is reduced a two-dimensional heat conduction problem in $x-z$ plane. The temperature of

the surrounding medium is denoted by a function T_f and assume its lower surface ($z = 0$) is held zero temperature.

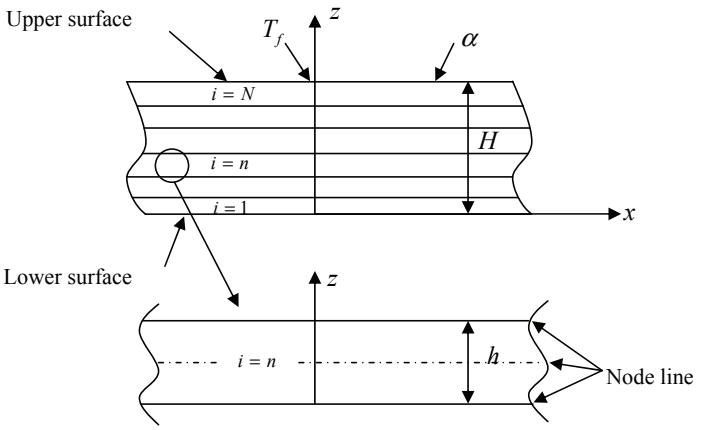

Figure 1: Analysis model and coordinate system

2.1 HNM for heat conduction problem

The thermal conductivity of the plate is assumed to take the following continuous form

$$\lambda(z) = \lambda_l + \frac{\lambda_u - \lambda_l}{H} z \; 0 \le z \le H \tag{1}$$

Where λ_u and λ_l are the thermal conductivity of upper and lower surfaces, respectively.

Specific heat c and density ρ are also assumed to be the continuous linear form just like the thermal conductivity. The heat conduction equation involving an internal heat source is taken as

$$\frac{\partial}{\partial x}[\lambda(z)\frac{\partial T}{\partial x}] + \frac{\partial}{\partial z}[\lambda(z)\frac{\partial T}{\partial z}] + q_v = c\rho\frac{\partial T}{\partial t} \tag{2}$$

The temperature field within a layer element is approximated as

$$T = \mathbf{N}(z)\mathbf{\Phi}(x,t) \tag{3}$$

where $\mathbf{N}(z)$ is a shape function matrix, and here the quadratic shape function is used as

$$\mathbf{N}(z) = [(1 - 3\bar{z} + 2\bar{z}^2)4(\bar{z} - \bar{z}^2)(2\bar{z}^2 - \bar{z})] \tag{4}$$

in which $\bar{z} = z/h$, h is thickness of a layer element. In Eq. (3), $\mathbf{\Phi}$ is a matrix consisting of nodal line temperatures, which are a function of the coordinate x and time t, and is denoted as

$$\mathbf{\Phi} = \begin{Bmatrix} \Phi_l \\ \Phi_m \\ \Phi_u \end{Bmatrix} \tag{5}$$

where the subscript l, m, u denotes lower, middle, upper nodal lines of an element. The initial condition and thermal boundary conditions are expressed as follows

$$T|_{t=0} = 0 \tag{6}$$

$$z = H;\ -\lambda(z)\frac{\partial T}{\partial z}\bigg|_{\Gamma} = \alpha(T_f - T)\big|_{\Gamma} \tag{7}$$

where Γ denotes the boundary of the plate.

Using the weighted residual method for Eq. (2) and Eq. (7), there have

$$\begin{aligned} &\int_0^h \mathbf{N}^T \left[c\rho\frac{\partial T}{\partial t} - [\frac{\partial}{\partial x}(\lambda(z)\frac{\partial T}{\partial x}) + \frac{\partial}{\partial z}(\lambda(z)\frac{\partial T}{\partial z})] - q_v \right] dz + \lambda(z)\frac{\partial T}{\partial z}\bigg|_{\Gamma} \\ &+ \alpha(T - T_f)\big|_{\Gamma} = 0 \end{aligned} \tag{8}$$

Performing lengthy and simple operations, we obtain

$$\mathbf{C}\dot{\mathbf{\Phi}} + \mathbf{K}_D\mathbf{\Phi} = \mathbf{Q} \tag{9}$$

Where

$$\mathbf{C} = \int_0^h \mathbf{N}^T c\rho\mathbf{N} dz \tag{10}$$

$$\mathbf{K}_D = -\int_0^h \mathbf{N}^T\lambda(z)\mathbf{N}dz \cdot \frac{\partial^2}{\partial x^2} + (\lambda(z)\frac{\partial \mathbf{N}}{\partial z}\bigg|_{\Gamma} + \alpha\mathbf{N}|_{\Gamma} - \int_0^h \mathbf{N}^T\lambda(z)\frac{\partial^2\mathbf{N}}{\partial z^2}dz) \tag{11}$$

$$\mathbf{Q} = \int_0^h \mathbf{N}^T q_v dz + \alpha T_f\big|_{\Gamma} \tag{12}$$

Substituting Eq. (4) into Eq. (10) and integrating along$z$, we obtain

$$\mathbf{C} = \frac{c\rho h}{30}\begin{bmatrix} 4 & 2 & -1 \\ 2 & 16 & 2 \\ -1 & 2 & 4 \end{bmatrix} \tag{13}$$

Performing simple operation to Eq. (11), $\mathbf{K}_D$ can be written as

$$\mathbf{K}_D = -\mathbf{A}_1 \cdot \frac{\partial^2}{\partial x^2} + \mathbf{A}_0 \tag{14}$$

where

$$\mathbf{A}_1 = \frac{h\lambda(z)}{30}\begin{bmatrix} 4 & 2 & -1 \\ 2 & 16 & 2 \\ -1 & 2 & 4 \end{bmatrix} \tag{15}$$

$$\mathbf{A}_0 = \frac{\lambda(z)}{3h}\begin{bmatrix} 7 & -8 & 1 \\ -8 & 16 & -8 \\ 1 & -8 & 7 \end{bmatrix} + \alpha \begin{bmatrix} 1 & 0 & 0 \\ 0 & 0 & 0 \\ 0 & 0 & -1 \end{bmatrix} \tag{16}$$

After lengthy and tedious operations to Eq. (12), we have

$$\mathbf{Q} = \frac{q_v h}{6}\begin{bmatrix} 1 \\ 4 \\ 1 \end{bmatrix} + \alpha T_f\big|_\Gamma \tag{17}$$

Assembling all elements, Eq. (9) becomes as

$$\mathbf{C}_s\dot{\mathbf{\Phi}}_s + \mathbf{K}_{Ds}\mathbf{\Phi}_s = \mathbf{Q}_s \tag{18}$$

where

$$\mathbf{K}_{Ds} = -\mathbf{A}_{1s} \cdot \frac{\partial^2}{\partial x^2} + \mathbf{A}_{0s} \tag{19}$$

where the subscript D denotes the matrix $\mathbf{K}_s$ is a differential operator matrix. Matrices $\mathbf{C}_s, \mathbf{A}_{is}(i = 1,2), \mathbf{Q}_s$ are obtained by assembling $\mathbf{C}, \mathbf{A}_i(i = 1,2), \mathbf{Q}$ for all the elements. Because the quadratic shape function is used, and there are three nodal lines in each element, the dimension of $\mathbf{C}_s, \mathbf{A}_{is}(i = 1,2)$ matrices are $M \times M(M = 2N + 1)$, the dimension of $\mathbf{Q}_s$ matrices is $M \times 1(M = 2N + 1)$, where $N$is the number of the layer element.

2.2 Fourier Transform

The Fourier transform of domain x to domain ζ_x can be defined as follows

$$\tilde{\mathbf{\Phi}}_s(\zeta_x, t) = \int_{-\infty}^{\infty} \mathbf{\Phi}_s(x,t) e^{i\zeta_x x} dx \tag{20}$$

The application of the Fourier transform to Eq. (16) leads to a set of system equations as follows

$$\mathbf{C}_s\dot{\tilde{\mathbf{\Phi}}}_s + \mathbf{K}_s\tilde{\mathbf{\Phi}}_s = \tilde{\mathbf{Q}}_s \tag{21}$$

where $\dot{\tilde{\mathbf{\Phi}}}_s, \tilde{\mathbf{\Phi}}_s$ and $\tilde{\mathbf{Q}}_s$ are the Fourier transform of $\dot{\mathbf{\Phi}}_s, \mathbf{\Phi}_s$ and $\mathbf{Q}_s$,respectively. Matrix $\mathbf{K}_s$ is given by

$$\mathbf{K}_s = \zeta_x^2\mathbf{A}_{1s} + \mathbf{A}_{0s} \tag{22}$$

Which is a constant matrix for given ζ_x.

2.3 Temperature in ζ_x Domain

Assume the corresponding homogeneous solution of Eq. (21) as

$$\tilde{\mathbf{\Phi}}_s = \boldsymbol{\psi} e^{-\omega t} \tag{23}$$

Instituting Eq. (23) into Eq. (21), obtain

$$[\mathbf{K}_s - \omega\mathbf{C}_s]\boldsymbol{\psi} = 0 \tag{24}$$

Its eigenvalue equation is obtained as

$$|\mathbf{K}_s - \omega\mathbf{C}_s| = 0 \tag{25}$$

From Eq.(25) and (24), eigenvalues $\omega_m (m = 1,2,\ldots,M)$ and corresponding eigenvectors $\boldsymbol{\psi}_m^R$ can be obtained.

Transformed $\tilde{\mathbf{\Phi}}_s$ and $\tilde{\mathbf{Q}}_s$ of Eq. (21) can be expressed as series of eigenvectors

$$\tilde{\mathbf{\Phi}}_s = \sum_{m=1}^{M} a_m \boldsymbol{\psi}_m^R \tag{26}$$

$$\tilde{\mathbf{Q}}_s = \sum_{m=1}^{M} b_m \mathbf{C}_s \boldsymbol{\psi}_m^R \tag{27}$$

where a_m, b_m are functions of time.

Substitution of Eqs. (26) and (27) into (19) leads to the following equation

$$\dot{a}_m + \omega_m a_m = b_m \tag{28}$$

In which b_m can be rewrite by Eq. (27) as follows

$$b_m = \frac{\boldsymbol{\psi}_m^L \tilde{\mathbf{Q}}_s}{\boldsymbol{\psi}_m^L \mathbf{C}_s \boldsymbol{\psi}_m^R} \tag{29}$$

Where superscripts L and R represent left eigenvector and right eigenvector, respectively.

For a given $\tilde{\mathbf{Q}}_s$, b_m can be obtained.

From the initial condition (6), we have

$$a_m|_{\tau=0} = 0 \tag{30}$$

Solving Eq. (28) for a_m, we obtain

$$a_m = e^{-\omega_m t}\left(\int \frac{\boldsymbol{\psi}_m^L \tilde{\mathbf{Q}}_s}{\boldsymbol{\psi}_m^L \mathbf{C}_s \boldsymbol{\psi}_m^R} e^{\omega_m t} dt + O\right) \tag{31}$$

When the internal heat source is not considered, $\mathbf{Q}_s$ can be rewritten as

$$\mathbf{Q}_s = \alpha T_f\big|_\Gamma \tag{32}$$

Here assume that $\mathbf{Q}_s$ has the following form

$$\mathbf{Q}_s = \begin{cases} \alpha T_{0f} \sin(\omega_f t)\big|_{\Gamma s} & t \le t' \\ 0 & t > t' \end{cases} \tag{33}$$

T_{0f} is a constant media temperature, t_1 is the control period for supplying heat.

Applying the Fourier transform to Eq. (33), we have

$$\tilde{\mathbf{Q}}_s = \begin{cases} \alpha \tilde{T}_{0f} \sin(\omega_f t)\big|_{\Gamma s} & t \le t' \\ 0 & t > t' \end{cases} \tag{34}$$

Instituting Eq. (34) into Eq. (31), a_m becomes as

$$a_m = e^{-\omega_m t}\left(\int \frac{\boldsymbol{\psi}_m^L\ \alpha \tilde{T}_{0f} \sin(\omega_f t)\big|_{\Gamma s}}{\mathbf{C}_c} e^{\omega_m t} dt + O\right) \tag{35}$$

In which

$$\mathbf{C}_c = \boldsymbol{\psi}_m^L \mathbf{C}_s \boldsymbol{\psi}_m^R \tag{36}$$

Instituting Eq. (30) into Eq. (35), then into Eq. (26), the temperature matrix in the Fourier transform domain is given as

$$\tilde{\boldsymbol{\Phi}}_s = \begin{cases} \sum_{m=1}^{M} \frac{\boldsymbol{\psi}_m^L\, \alpha \tilde{T}_{0f}\big|_{\Gamma s} \boldsymbol{\psi}_m^R}{(\omega_f^2+\omega_m^2)\mathbf{C}_c} (\omega_m \sin(\omega_f t) - \omega_f \cos(\omega_f t) + \omega_f e^{-\omega_m t}) & t \le t' \\ \sum_{m=1}^{M} e^{-\omega_m t} \cdot \frac{\boldsymbol{\psi}_m^L\, \alpha \tilde{T}_{0f}\big|_{\Gamma s} \psi_m^R \cdot \{[\omega_m \sin(\omega_f t_1) - \omega_f \cos(\omega_f t_1)] e^{\omega_m t_1} + 2\omega_f\}}{(\omega_f^2+\omega_m^2)\mathbf{C}_c} & t > t' \end{cases} \tag{37}$$

2.4 Temperature in Space-Time Domain

Performing the inverse Fourier transform of Eq.(37), the temperature in the space-time domain can be expressed as

$$\mathbf{\Phi}_s(x,t) = \frac{1}{2\pi}\int_{-\infty}^{\infty} \tilde{\mathbf{\Phi}}_s(\zeta_x,t)e^{-i\zeta_x x}d\zeta_x \tag{38}$$

The integration in Eq. (38) can be carried out using fast Fourier transform (FFT) techniques.

3 Results and Discussions

In computation, time interval is taken as 1 second and control period t' is 0.5 second. The time domain is divided into 200 steps. The wave number domain is taken as from 0 to 64π and is divided into 750 steps. Space domain is taken as from 0 to 10 and is divided into 1000 steps. Ceramic ZrO_2 and metal Ti - 6Al - 4V are taken in investigation. The material properties of ZrO_2 and Ti - 6Al - 4V are shown in table 1. Upper and lower surface consist of ZrO_2 and Ti - 6Al - 4V, respectively. The properties of the middle materials vary continuously along its thickness direction.

Table 1: Material properties of ZrO_2 and Ti - 6Al - 4V

Material	Thermal conductivity $\lambda(\mathrm{W\cdot m^{-1}\cdot K^{-1}})$	Specific heat $\mathrm{J\cdot kg^{-1}\cdot K^{-1}}$	Density $\rho(\mathrm{kg\cdot m^{-3}})$
ZrO_2	2.09	456.7	5331
Ti - 6Al - 4V	7.50	537.0	4420

In computation, the following dimensionless parameters are introduced

$$\bar{T} = T/T_0, \quad \bar{t} = t/t_0, \quad \bar{x} = x/H,$$

$$\bar{\lambda} = \lambda/\lambda_0, \quad \bar{c} = c/c_0, \quad \bar{\rho} = \rho/\rho_0, \quad \bar{\alpha} = \alpha/\alpha_0 \tag{39}$$

The temperature distribution of FGM plate subjected to the transient surrounding heat of Eq. (33) is computed using HNM at different time step. Dividing FGM plate into different elements such as 20,40,80,100, the temperature distribution of the upper surface for FGM plate at 80 step, that is 0.4 second, corresponding having heat supply, are shown in Fig.2. From Fig.2, it can be seen, while 20 elements and 40 elements are divided, the temperature distributions are obvious difference; while 40 elements and 80 elements are divided, the results are very approaching; while 80 elements and 100 elements are divided, the results are almost coincidence. This

shows the presented method is convergent. The better results can be obtained while the element is smaller enough. For saving computation time and ensuring the result precision, the 40 elements are used in the following computation.

The temperature distributions at three positions are shown from Fig. 3 to Fig. 5. The three positions are upper surface, middle surface and lower surface, respectively. Three observation times are considered, $t1$ time, $t2$ time and $t3$ time.$t1 = 0.4$s, $t2 = 0.51$s, $t3 = 0.52$s. The heat supply time is $t' = 0.5$s, $t1$ time corresponds to the state of heat supply, $t2$ time and $t3$ time correspond to the state of without heat supply. From Fig.3, it can be seen that the wave character of the temperature distribution appeared on the upper surface of FGM plate while far from heat source at $t1$ time. The reason is the heat source supplying to the plate with sine form. The decrease character also appeared while far from heat source. In a word, at $t1$ time the regular of the temperature distribution of the upper surface for FGM plate is that the temperature distribution appeared wave decrease character while far from heat source with sine heat supply. At $t2$ time and $t3$ time, the decrease character of temperature distribution existed, yet the wave character vanished. The reason is this time corresponding to the state of without heat supply. Free heat conduction proceeded at that time. So the temperature on the upper plate appeared the smooth decrease character while without heat supply. We can also know that the temperature on the upper surface anywhere at $t2$ time is higher than at $t3$ time. The temperature decreased without heat supply and it will decrease to zero by a long time as if it returned initial time state. We can also find the highest temperature is not at heat source position. It appeared wave crest position near heat source firstly because of the sine heat supply.

Observing the temperature distribution for middle surface and lower surface of the FGM plate such as Fig.4 and Fig.5, the same regular can be obtained, that is wave decrease character for having heat supply and smooth decrease character for without heat supply. Comparing Fig.3, Fig.4 and Fig5, we can found that the only different is the temperature value. The thicker plate, the lower temperature, the highest temperature is 0.24 on upper surface while only 0.0009 on the lower surface at $t1$ time for the state of having heat source.

Temperature distribution of time histories of FGM plate on the different observation surface subjected to transient heat supply is shown from Fig. 6 to Fig. 8. Three observation positions are chosen for studying. They are point $x1$, point $x2$ and point $x3$, respectively. Here, $x1 = 0.1$, $x2 = 0.5$, $x3 = 1$. While supplying transient heat source, the temperature distribution regular of the three observation position is that the temperature of point $x1$ is higher than point $x2$, the temperature of point $x2$ is higher than point $x3$. This shows the nearer heat source, the higher temperature, vice versa. It agrees with the actual results. Observing the temperature of the

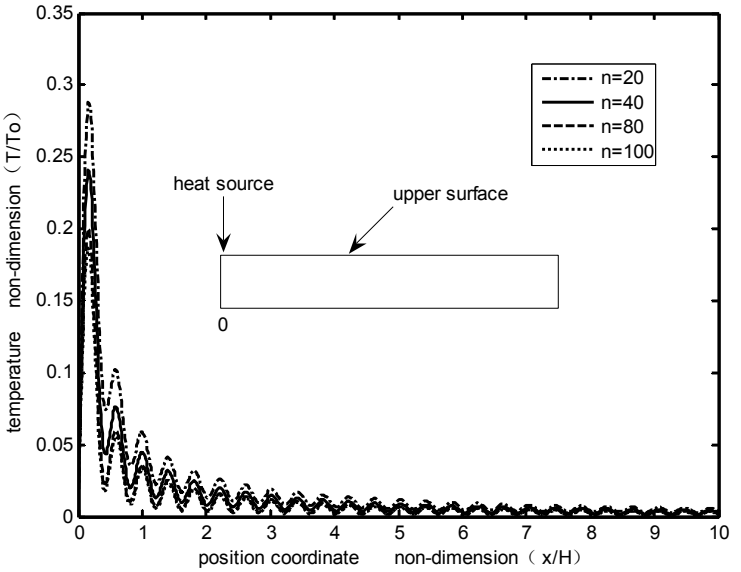

Figure 2: Temperature distribution of the upper surface for FGM plate divided different element

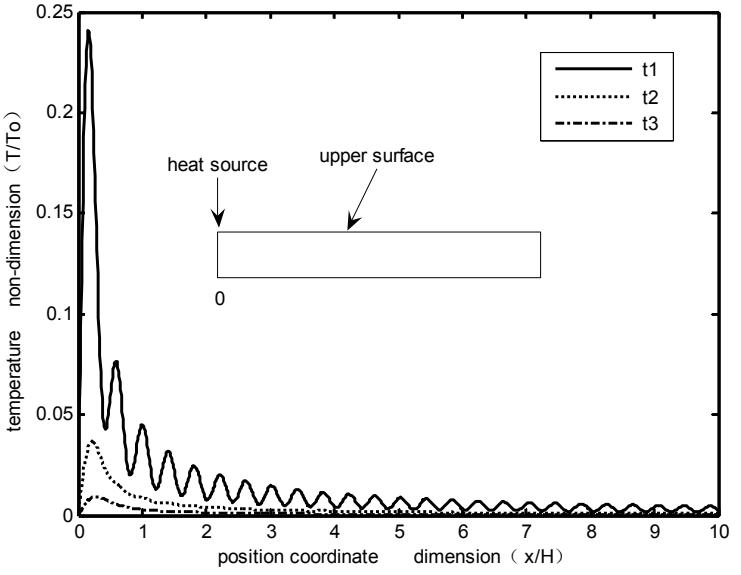

Figure 3: Temperature distribution of the upper surface of FGM plate in different times subjected to sine transient heat supply

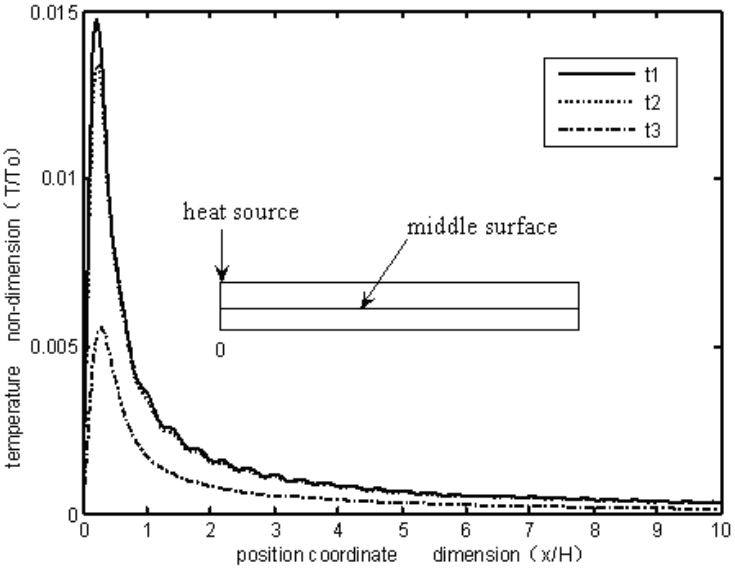

Figure 4: Temperature distribution of the middle surface of FGM plate in different times subjected to sine transient heat supply

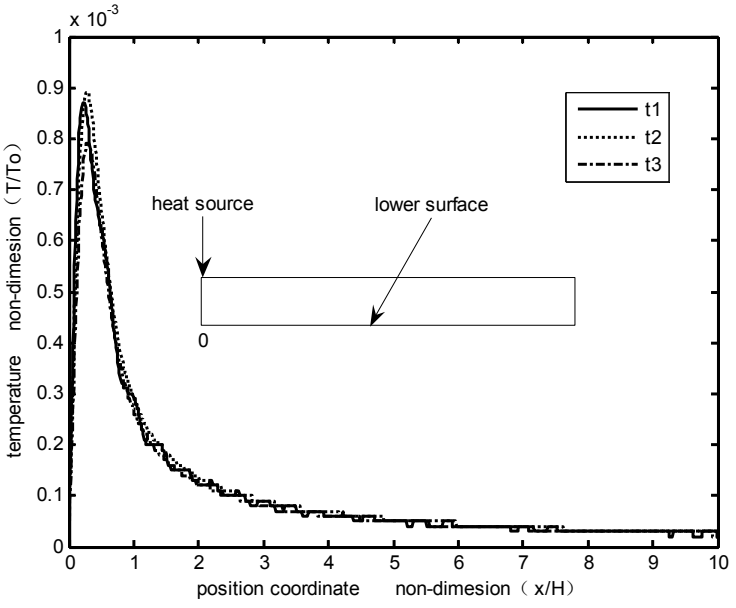

Figure 5: Temperature distribution of the lower surface of FGM plate in different times subjected to sine transient heat supply

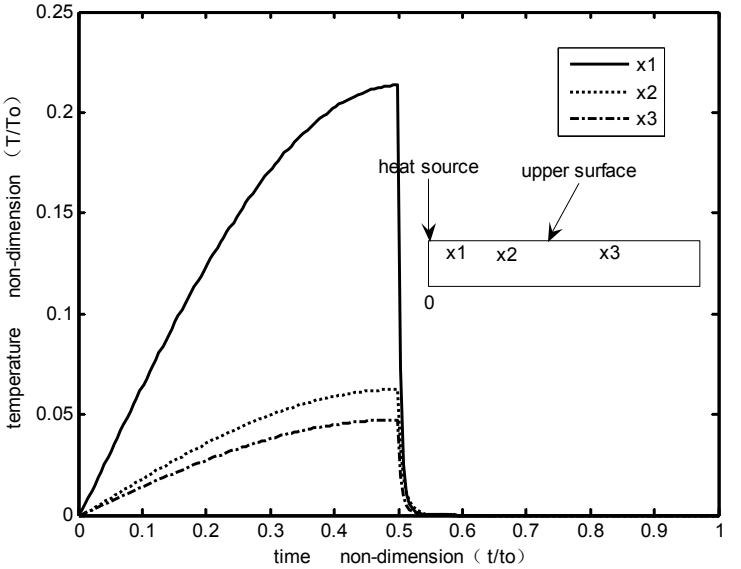

Figure 6: Temperature distribution of time histories of the different observation position in the upper surface of FGM plate subjected to sine transient heat supply

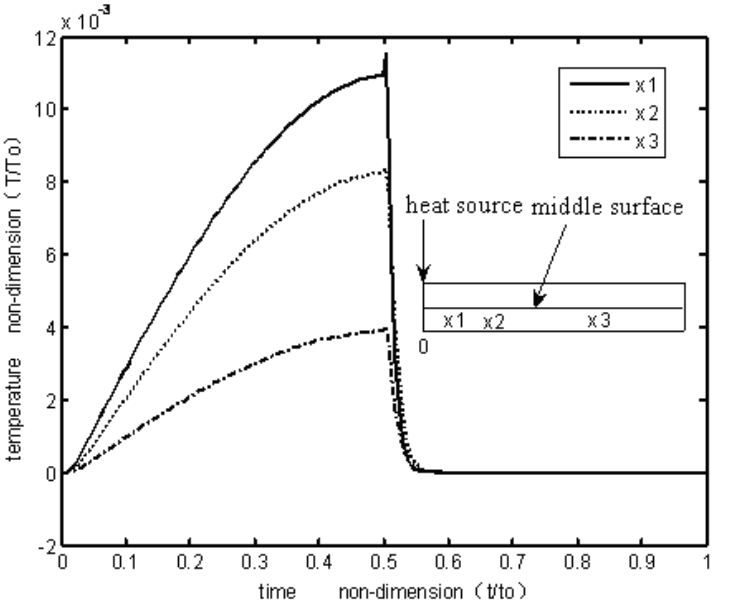

Figure 7: Temperature distribution of time histories of the different observation position in the middle surface of FGM plate subjected to sine transient heat supply

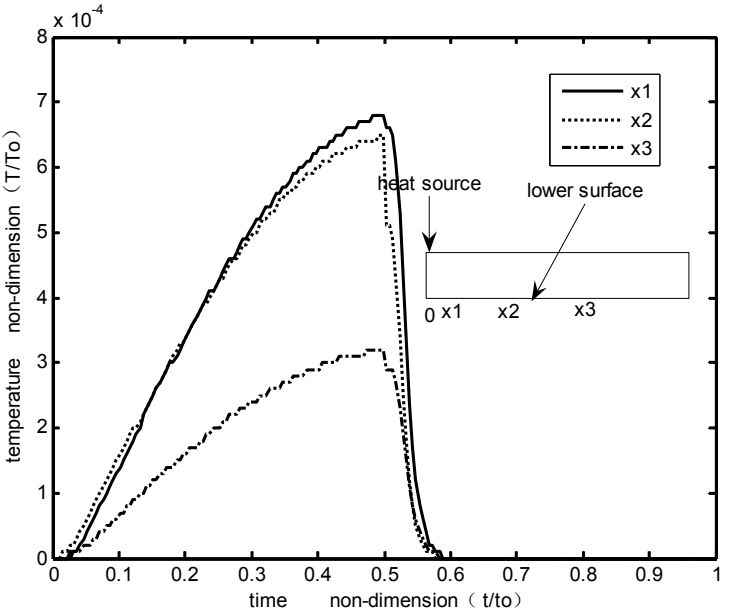

Figure 8: Temperature distribution of time histories of the different observation position in the lower surface of FGM plate subjected to sine transient heat supply

upper surface at point $x1$, we can found that the temperature distribution of the plate is sine form at from 0s to 0.5s for having heat supply, then having inflection temperature and appearing sudden decline after 0.5s for without heat supply. The temperature decreased to zero in a short time 0.15s just as returning to initial time state. It shows that the transient free heat conduction proceeded while without heat source. The phenomena of point $x2$ and $x3$ is just as point $x1$. The phenomena of else surface is just as upper surface. It also shows that the transient heat conduction time is from 0.5s to 0.58s whether observation position is far or near from the heat source. The variation trend of temperature distribution is almost same on the different observation surface. The only difference is the temperature value.

4 Conclusions

In the present article, the transient heat conduction of FGM plate has been investigated using the HNM. The temperature distribution of the FGM plate along the thickness direction and length direction are shown. This study applies HNM into transient heat conduction and obtained useful result. The application domain of HNM is extends to transient heat domain and presents a new way to investigate the

transient heat problem.

Acknowledgement: This research work was supported by the National Science Fund for Distinguished Young Scholars (grant No 10725208), the Ph.D. Programs Foundation of Ministry of Education of China (grant No 20070532021), National Basic Research Priorities Program of China (grant No A1420080166), the Science & Technology Major Project for High Numerical Control Machine and Basic Manufacture Equipment (grant No 2009ZX04001-091)

References

Liu, C.-S. (2008): The lie-group shooting method for thermal stress evaluation through an internal temperature measurement. *CMC: Computers, Materials & Continua*, vol.8, no.1, pp.1-16.

Cheng, Z.Q.; Batra, R.C. (2000): Three-dimensional thermoelastic deformations of a functionally graded elliptic plate. *Composites: Part B*, 31, 97-106.

Glaysar, C.; Valerie, G. (2002): Maximum of entropy and extension of covariance matrices for eriodically correlated and multivariate process. *Journal of Wind Engineering and Industrial Aerodynamics*, vol.59, pp.37-52.

Liu, G.R.; Xi, Z.C. (2002): *Elastic waves in anisotropic laminates*. CRC PRESS.

Lutz, M.P.; Zimmerman, R.W. (1996): Thermal stresses and effective thermal expansion coefficient of a functionally gradient sphere. *J Therm Stress*, vol.19, pp.39–54.

Ootao, Y.; Tanigawa, Y. (2002): Transient thermal stresses of angle-ply laminated cylindrical panel due to nonuniform heat supply in the circumferential direction. *Composite structures*, vol.55, pp.95-103.

Qian, L.F.; Batra, R.C. (2004): Transient thermoelastic deformations of a thick functionally graded plate. *Journal of Thermal Stresses*, vol.27, pp.705–740.

Qian, L.F.; Batra, R.C.; Chen, L.M. (2004): Analysis of cylindrical bending thermoelastic deformations of functionally graded plates by a meshless local Petrov–Galerkin method. *Computational Mechanics*, vol.33, pp.263–273.

Reddy, J.N.; Cheng, Z.Q. (2001): Three-dimensional thermomechanical deformations of functionally graded rectangular plates. *European Journal of Mechanics A/Solids*, vol.20, pp. 841–855.

Savoia, M. ; Reddy, J.N. (1995): Three-dimensional thermal analysis of laminated composite plates. *Int. J. Solids Structures*, vol.32, pp.593-608.

Sladek, J.; Sladek,V.; Solek, P.; Wen, P.H.; Atluri, S.N. (2008a): Thermal Analysis of Reissner-Mindlin Shallow Shells with FGM Properties by the MLPG. *CMES:*

Computer Modeling in Engineering and Sciences, vol.30, no.2, pp.77-97.

Sladek, J.; Sladek,V.; Tan, C.L.; Atluri, S.N. (2008b): Analysis of Transient Heat Conduction in 3D Anisotropic Functionally Graded Solids, by the MLPG Method. *CMES: Computer Modeling in Engineering and Sciences*, vol.32, no.3, pp.161-174.

Tian, J.H.; Han, X.; Long, S.Y.; Xie G.Q. (2009): An Analysis of the Heat Conduction Problem for Plates with the Functionally Graded Material Using the Hybrid Numerical Method. *CMC: Computers, Materials & Continua*, vol. 10, no.3, pp.229-242.

Vel, S.S.; Batra, R.C. (2002): Exact thermoelasticity solution for functionally graded thick rectangular plates. *AIAA Journal*, vol.40, pp.1421–1433.

Vel, S.S.; Batra, R.C. (2003a): Three-dimensional analysis of transient thermal stresses in functionally graded plates. *International Journal of Solids and Structures*, vol.40, pp.7181–7196.

Vel, S.S.; Batra, R.C. (2003b): Exact thermoelasticity solution for cylindrical bending deformations of functionally graded plates. In: Proceedings of IUTAM Symposium on Dynamics of Advanced Materials and Smart Structures, Yonezawa, Japan, 20–24 May 2002. In: Watanabe, K, Ziegler, F. (Eds.), Dynamics of Advanced Materials and Smart Structures. Kluwer Academic Publishers, Dordrecht.

Zimmerman, R.W.; Lutz, M.P. (1999): Thermal stresses and thermal expansion in a uniformly heated functionally graded cylinder. *J Therm Stress*, vol.22, pp.177–88.